Measurements of Beam Shape Coefficients in Generalized Lorenz-Mie Theory and the Density-Matrix Approach. Part 1: Measurements

Gérard Gouesbet*

(Received: 4 March 1996)

Abstract

Up to now, beam shape coefficients, g_n or g_n^m, encoding an illuminating beam in generalized Lorenz-Mie theory have been derived from *a priori* theoretical electromagnetic descriptions. It is shown that, from intensity measurements in the laboratory, one can measure so-called density matrices associated with the beam shape coefficients. In the case of axisymmetric beams, when the beam is encoded by a set of special beam shape coefficients, g_n, one has to consider one matrix, I_{nm}. In the general case, i.e. when the beam is encoded by a double set of coefficients, $g_{n,TM}^m$, $g_{n,TE}^n$, one can measure three 4D matrices, M_{np}^{mq}, E_{np}^{mq}, C_{np}^{mq}. Measuring such matrices from an actual beam in a laboratory and using them in the density matrix approach to the generalized Lorenz-Mie theory would allow a better characterization of the scattering phenomena occurring when a scatter center is illuminated by an arbitrary-shaped beam, therefore opening up new opportunities for refined particle characterization.

1 Introduction

Recent advances in light scattering theory result from the generalized Lorenz-Mie theory (GLMT) describing the interaction between a spherical particle (homogeneous or multilayered) and an illuminating arbitrary-shaped beam (see Refs. [1, 2] and references therein). In GLMT, the illuminating beam is described by partial wave expansions whose coefficients are named beam shape coefficients (BSCs). In the general case (arbitrary-shaped beams), the BSCs form a double set $\{g_{n,TM}^m, g_{n,TE}^m\}$, in which n ranges from 1 to infinity, m from $(-n)$ to $(+n)$, and TM, TE stand for transverse magnetic and transverse electric, respectively. When the beam is axisymmetric, such as for on-axis Gaussian beams, this double set reduces to a single set $\{g_n\}$ of special BSCs [3]. All quantities arising in GLMT such as scattered fields and intensities, or cross-sections, are expressed in terms of the BSCs, which are therefore ubiquitous in this theoretical framework [4].

The BSCs can be theoretically evaluated when the expressions for the radial electric and magnetic fields (E_r and H_r, respectively) are known. Therefore, up to now, evaluations of BSCs relied on *a priori* theoretical descriptions of the beam under study (see Refs. [5–7] and references therein for the case of Gaussian beams, Refs. [8–10] for the case of laser sheets and Ref. [11] for top-hat beams). Unfortunately, an actual beam in a laboratory may depart from its ideal *a priori* theoretical description, therefore possibly inducing some difficulties in accurately interpreting experimental data, as exemplified in Ref. [12].

In such a case, when scattering data are used for optical particle characterization, inaccuracies may arise because the *a priori* theoretical description of the beam does not correspond to the actual beam used in the experiments. In order to open up new opportunities for refined particle characterization, it is desirable to measure BSCs of the actual beam under study rather than deducing them from a theoretical description. This is the issue discussed in this paper.

Solving this issue may be not urgent in many cases. However, the data exhibited in Ref. [12] clearly show that, in other cases, there is no way to understand definitely some scattering experiments (and associated particle characterizations) if the issue is not solved. Furthermore, manipulations of beams in optical designs tend to become more complex with the obvious forecast that the issue under study is certainly going to become crucial as soon as the opportunity to measuring BSCs of an actual beam in a laboratory is offered.

It is also of interest to note that here we are facing an inverse problem. The direct problem may be stated as being, in a GLMT framework, the ''exercise'' of determining scattering properties, such as local beam intensities, knowing the spectrum of BSCs. The inverse problem discussed here is more challenging: it amounts to using measured beam intensities to determine the BSCs.

The paper is organized as follows. Section 2 recalls properties of so-called axisymmetric beams for which the BSCs reduce to a set of coefficients g_n. Section 3 discusses the possibility of measuring BSCs by experimentally investigating field components. Section 4 examines how the situation is modified when we rely on intensity measurements rather than on field measurements. Section 5 similarly discusses the general case when the beam is encoded by a double set $\{g_{n,TM}^m, g_{n,TE}^m\}$ of BSCs rather than by a single set $\{gn\}$.

2 Properties of Axisymmetric Beams

We consider a monochromatic electromagnetic wave with time dependence $\exp(i\omega t)$, where ω is the angular frequency. This term will hereafter be omitted in all equations as is the normal practice.

* Prof. *G. Gouesbet*, Laboratoire d'Énergétique des Systèmes et Procédés, INSA de Rouen, URA CNRS 230, B.P. 08, F-76131 Mont Saint Aignan Cedex (France).

0934-0866/97/0102-0012 $17.50+.50/0

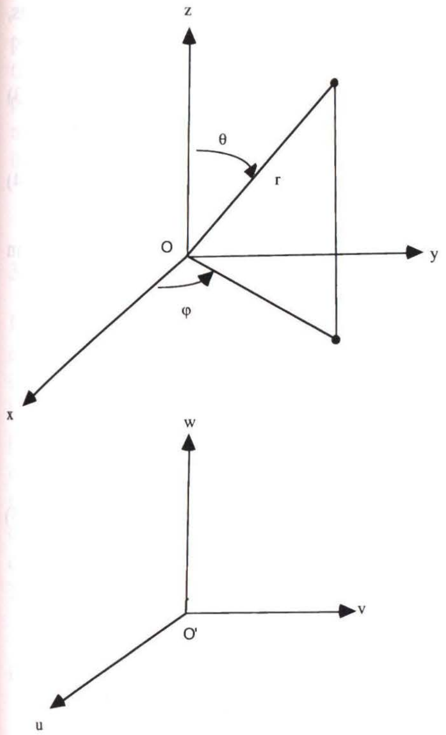

Fig. 1: Coordinate systems.

The beam is described in a spherical coordinate system (r, θ, φ) attached to a Cartesian coordinate system (Oxyz). When scattering by a sphere is under study, O is the center of the sphere (Figure 1). Under such conditions, the incident beam may be described by the two Bromwich scalar potentials (BSPs) [4]:

$$U_{TM} = E_0 r \sum_{n=1}^{\infty} \sum_{m=-n}^{+n} c_n^{pw} g_{n,TM}^m \Psi_n^1(kr) P_n^{|m|}(\cos\theta) e^{im\varphi} \tag{1}$$

$$U_{TE} = H_0 r \sum_{n=1}^{\infty} \sum_{m=-n}^{+n} c_n^{pw} g_{n,TE}^m \Psi_n^1(kr) P_n^{|m|}(\cos\theta) e^{im\varphi} \tag{2}$$

in which $g_{n,TM}^m$ and $g_{n,TE}^m$ are the BSCs, $\Psi_n^1(kr)$ are spherical Bessel functions and $P_n^{|m|}(\cos\theta)$ are associated Legendre polynomials. Arguments (kr), in which k is the wavenumber, and ($\cos\theta$) will be omitted most of the time from now on, for convenience. Coefficients c_n^{pw}, in which pw stands for "plane wave", are the expansion coefficients of a plane wave in the Bromwich formulation. They are expressed as [4, 13]

$$c_n^{pw} = \frac{1}{ik}(-i)^n \frac{2n+1}{n(n+1)}. \tag{3}$$

When scattering by a sphere is under study, we commonly use a second coordinate system (O'uvw), with axes parallel to the axes of the particle coordinate system (Oxyz), attached to the beam (Figure 1). For instance, if the illuminating beam is a Gaussian beam, O' should preferably be the beam waist center and the beam would propagate along O'w (standardly towards positive ws). It then appears that BSCs are specific to a given particle location. Therefore, they depend on the structure of the laser beam in addition to the particle location.

Instead of using spherical Bessel functions $\Psi_n^1(kr)$, we may also use Ricatti-Bessel functions, defined by

$$\Psi_n(kr) = kr\Psi_n^1(kr). \tag{4}$$

Then, the Bromwich scalar potentials may be rewritten as

$$U_{TM} = \frac{E_0}{k} \sum_{n=1}^{\infty} \sum_{m=-n}^{+n} c_n^{pw} g_{n,TM}^m \Psi_n P_n^{|m|} e^{im\varphi} \tag{5}$$

$$U_{TE} = \frac{H_0}{k} \sum_{n=1}^{\infty} \sum_{m=-n}^{+n} c_n^{pw} g_{n,TE}^m \Psi_n P_n^{|m|} e^{im\varphi}. \tag{6}$$

Field components in spherical coordinates may subsequently be derived from the BSPs by using rules of derivation [4, 13] that we here symbolically write as

$$x_i = f_i^x(U_{TM}, U_{TE}). \tag{7}$$

We also consider the intensities flowing in the x-, y- and z-directions given by the components S_x, S_y and S_z of the Poynting vector, respectively, according to

$$\begin{pmatrix} S_x \\ S_y \\ S_z \end{pmatrix} = \frac{1}{2} \mathrm{Re} \begin{pmatrix} E_y H_z^* - E_z H_y^* \\ E_z H_x^* - E_x H_z^* \\ E_x H_y^* - E_y H_x^* \end{pmatrix} \tag{8}$$

where $E_x, \ldots, H_z$ are the Cartesian electric and magnetic field components, and the asterisks denote complex conjugates.
As in Ref. [3], we now define an axisymmetric beam to be a beam for which S_z does not depend on φ, in suitably chosen coordinate systems. The best example of an axisymmetric-shaped beam (apart from the trivial plane wave) is a Gaussian laser beam. Although this is the terminology introduced in Ref. [3], it may be misleading in the present context. To be more specific, axisymmetric formulation requires not only the laser beam to be axisymmetric but also the coordinate center O to be located on the axis of symmetry. We may therefore better refer to this situation as corresponding to an axisymmetric on-axis illumination. It is then shown that BSCs of a (generic) axisymmetric beam satisfy [3]

$$\left.\begin{array}{c} g_n^m = 0, |m| \neq 1 \\ g_{n,TM}^1 = \frac{1}{K} g_{n,TM}^{-1} = -i\epsilon g_{n,TE}^1 = i\frac{\epsilon}{K} g_{n,TE}^{-1} \neq 0 \end{array}\right\}. \tag{9}$$

In Eq. (9), $\epsilon = \pm 1$, depending on the direction of propagation of the beam. More specifically, we have $\epsilon = -1$ (+1) when the energy flux flows towards positive z (negative z). Since the direction of the energy flux may trivially be determined for an actual beam in the laboratory, we take $\epsilon = -1$ from now on [3]. The other constant K (which must be a real number) determines the state of polarization of the light and, therefore, will be called the polarization parameter. More specifically, it is shown that, for a given K, we have a linear combination of two polarization states, one for which E_r is proportional to $\cos\phi$ and one for which it is proportional to $\sin\phi$, in a suitably chosen coordinate system with azimuthal angle ϕ. Nonmixed states of polarization correspond to $K = \pm 1$ (see Ref. [3]). The usual expression for on-axis Gaussian beams [13, 14] polarized in the x-direction at the focal waist are recovered from Eq. (9) with $K = 1$, $\epsilon = -1$.

From Eq. (9), we then see that the double set of BSCs $g^m_{n,TM}$, $g^m_{n,TE}$ reduces to a single set of special BSCs g_n that we define as

$$g_n = 2g^1_{n,TM}. \tag{10}$$

From Eqs. (1), (2) and (9), the BSPs for an axisymmetric beam propagating in the z-direction are then found to reduce to

$$U_{TM} = \frac{E_0 r}{2}(e^{1\varphi} + Ke^{-1\varphi})\sum_{n=1}^{\infty} c_n^{pw} g_n \Psi_n^1 P_n^1 \tag{11}$$

$$U_{TE} = \frac{H_0 r}{2i}(e^{1\varphi} - Ke^{-1\varphi})\sum_{n=1}^{\infty} c_n^{pw} g_n \Psi_n^1 P_n^1. \tag{12}$$

We introduce effective BSCs:

$$G_n = E_0 g_n \tag{13}$$

and recall that

$$k = \omega\epsilon_0 \frac{E_0}{H_o} = \omega\mu_0 \frac{H_0}{E_0} \tag{14}$$

where ϵ_0 and μ_0 are the electric and magnetic capacities of the free space in which the beam propagates, respectively. Then the BSPs may be expressed in terms of G_ns in such a way that the strengths E_0 and H_0 of the electric and magnetic fields disappear:

$$U_{TM} = \frac{r}{2}(e^{i\varphi} + Ke^{-i\varphi})\sum_{n=1}^{\infty} c_n^{pw} G_n \Psi_n^1 P_n^1 \tag{15}$$

$$U_{TE} = \frac{-ik}{\omega\mu_0}\frac{r}{2}(e^{i\varphi} - Ke^{-i\varphi})\sum_{n=1}^{\infty} c_n^{pw} G_n \Psi_n^1 P_n^1. \tag{16}$$

The rules of derivation of Eq. (7) then allow one to express the field components in spherical coordinates according to

$$E_r = \frac{1}{2r}(e^{i\varphi} + Ke^{-i\varphi})\sum_{n=1}^{\infty} c_n^{pw} G_n n(n+1)\Psi_n^1 P_n^1 \tag{17}$$

$$E_\theta = \frac{1}{2r}(e^{i\varphi} + Ke^{-i\varphi})\sum_{n=1}^{\infty} c_n^{pw} G_n \left(\frac{dr\Psi_n^1}{dr}\tau_n - ikr\Psi_n^1\pi_n\right) \tag{18}$$

$$E_\varphi = \frac{i}{2r}(e^{i\varphi} - Ke^{-i\varphi})\sum_{n=1}^{\infty} c_n^{pw} G_n \left(\frac{dr\Psi_n^1}{dr}\pi_n - ikr\Psi_n^1\tau_n\right) \tag{19}$$

$$H_r = \frac{-i}{2r}\frac{k}{\omega\mu_0}(e^{i\varphi} - Ke^{-i\varphi})\sum_{n=1}^{\infty} c_n^{pw} G_n n(n+1)\Psi_n^1 P_n^1 \tag{20}$$

$$H_\theta = \frac{-i}{2r}\frac{k}{\omega\mu_0}(e^{i\varphi} - Ke^{-i\varphi})\sum_{n=1}^{\infty} c_n^{pw} G_n \left(\frac{dr\Psi_n^1}{dr}\tau_n - ikr\Psi_n^1\pi_n\right) \tag{21}$$

$$H_\varphi = \frac{1}{2r}\frac{k}{\omega\mu_0}(e^{i\varphi} + Ke^{-i\varphi})\sum_{n=1}^{\infty} c_n^{pw} G_n \left(\frac{dr\Psi_n^1}{dr}\pi_n - ikr\Psi_n^1\tau_n\right) \tag{22}$$

where $\pi_n = \pi_n(\cos\theta)$ and $\tau_n = \tau_n(\cos\theta)$ are Legendre functions, defined as

$$\pi_n = \frac{P_n^1}{\sin\theta} \tag{23}$$

$$\tau_n = \frac{dP_n^1}{d\theta}. \tag{24}$$

From Eqs. (17)–(22), we may then readily derive the Cartesian field components:

$$\begin{aligned} E_x = \frac{1}{2r}\sum_{n=1}^{\infty} c_n^{pw} G_n \Bigg\{ & \sin\theta\cos\varphi(e^{i\varphi} + Ke^{-i\varphi})n(n+1)\Psi_n^1 P_n^1 \\ & + \cos\theta\cos\varphi(e^{i\varphi} + Ke^{-i\varphi})\left(\frac{dr\Psi_n^1}{dr}\tau_n - ikr\Psi_n^1\pi_n\right) \\ & - i\sin\varphi(e^{i\varphi} - Ke^{-i\varphi})\left(\frac{dr\Psi_n^1}{dr}\pi_n - ikr\Psi_n^1\tau_n\right)\Bigg\} \end{aligned} \tag{25}$$

$$\begin{aligned} E_y = \frac{1}{2r}\sum_{n=1}^{\infty} c_n^{pw} G_n \Bigg\{ & \sin\theta\sin\varphi(e^{i\varphi} + Ke^{-i\varphi})n(n+1)\Psi_n^1 P_n^1 \\ & + \cos\theta\sin\varphi(e^{i\varphi} + Ke^{-i\varphi})\left(\frac{dr\Psi_n^1}{dr}\tau_n - ikr\pi_n\Psi_n^1\right) \\ & + i\cos\varphi(e^{i\varphi} - Ke^{-i\varphi})\left(\frac{dr\Psi_n^1}{dr}\pi_n - ikr\tau_n\Psi_n^1\right)\Bigg\} \end{aligned} \tag{26}$$

$$\begin{aligned} E_z = \frac{1}{2r}(e^{i\varphi} + Ke^{-i\varphi})\sum_{n=1}^{\infty} c_n^{pw} G_n \Bigg[& \cos\theta n(n+1)\Psi_n^1 P_n^1 \\ & - \sin\theta\left(\frac{dr\Psi_n^1}{dr}\tau_n - ikr\pi_n\Psi_n^1\right)\Bigg] \end{aligned} \tag{27}$$

$$\begin{aligned} H_x = \frac{-i}{2r}\frac{k}{\omega\mu_0}\sum_{n=1}^{\infty} c_n^{pw} G_n \Bigg\{ & \sin\theta\cos\varphi(e^{i\varphi} - Ke^{-i\varphi})n(n+1)\Psi_n^1 P_n^1 \\ & + \cos\theta\cos\varphi(e^{i\varphi} - Ke^{-i\varphi})\left(\frac{dr\Psi_n^1}{dr}\tau_n - ikr\Psi_n^1\pi_n\right) \\ & - i\sin\varphi(e^{i\varphi} + Ke^{-i\varphi})\left(\frac{dr\Psi_n^1}{dr}\pi_n - ikr\Psi_n^1\tau_n\right)\Bigg\} \end{aligned} \tag{28}$$

$$\begin{aligned} H_y = \frac{-i}{2r}\frac{k}{\omega\mu_0}\sum_{n=1}^{\infty} c_n^{pw} G_n \Bigg\{ & \sin\theta\sin\varphi(e^{i\varphi} - Ke^{-i\varphi})n(n+1)\Psi_n^1 P_n^1 \\ & + \cos\theta\sin\varphi(e^{i\varphi} - Ke^{-i\varphi})\left(\frac{dr\Psi_n^1}{dr}\tau_n - ikr\Psi_n^1\pi_n\right) \\ & + i\cos\varphi(e^{i\varphi} + Ke^{-i\varphi})\left(\frac{dr\Psi_n^1}{dr}\pi_n - ikr\Psi_n^1\tau_n\right)\Bigg\} \end{aligned} \tag{29}$$

$$\begin{aligned} H_z = \frac{-i}{2r}\frac{k}{\omega\mu_0}(e^{i\varphi} - Ke^{-i\varphi})\sum_{n=1}^{\infty} c_n^{pw} G_n \Bigg[& \cos\theta n(n+1)\Psi_n^1 P_n^1 \\ & - \sin\theta\left(\frac{dr\Psi_n^1}{dr}\tau_n - ikr\Psi_n^1\pi_n\right)\Bigg]. \end{aligned} \tag{30}$$

3 Measuring BSCs from Fields

We assume that we are faced with a beam in the laboratory for which we have checked that it is axisymmetric (on-axis), with axis z chosen in such a way that the energy flux propagates towards positive z ($\epsilon = -1$). We then have to measure the effective BSC G_ns and, furthermore, we also need actually to measure the polarization parameter K. We also assume that we are able to measure fields, both in amplitude and phase, such as by using interferometric/holographic techniques.

3.1 Using Spherical Components

First, we consider measurements of K and G_ns by relying on field components in spherical coordinates. These components are not independent in so far as they are linked by Maxwell's equations, leading to some amount of redundancy in the available information. Therefore, because BSCs are theoretically evaluated from components E_r and H_r, we here give due importance to these radial field components. Also, because effective BSC G_ns do not distinguish between TM and TE fields, we may choose to concentrate only on E_r.
Then from Eq. (17), we have

$$E_r(\varphi = 0) = \frac{K+1}{2r} \sum_{n=1}^{\infty} c_n^{pw} G_n n(n+1) \Psi_n^1 P_n^1 \tag{31}$$

$$E_r(\varphi = \frac{\pi}{2}) = \frac{i(1-K)}{2r} \sum_{n=1}^{\infty} c_n^{pw} G_n n(n+1) \Psi_n^1 P_n^1. \tag{32}$$

We then choose values of r and θ such that the r.h.s.s are finite in Eqs. (31)–(32) and define

$$R = \frac{E_r(\varphi = \frac{\pi}{2})}{E_r(\varphi = 0)} = \frac{i(1-K)}{K+1} \tag{33}$$

leading to

$$K = \frac{i-R}{i+R}. \tag{34}$$

Measuring the field ratio R therefore allows one to determine the polarization parameter K. For instance, let us consider the trivial example of an on-axis Gaussian beam for which $K = 1$, $\epsilon = -1$ in Eq. (9), such as discussed in Refs. [13, 14]. We then have E_r ($\varphi = \pi/2) = 0$ from Eq. (32), leading to $R = 0$. If we study an on-axis Gaussian beam in the laboratory, we then would measure $R = 0$ which, from Eq. (34), implies $K = 1$, as it should.
Next, let us set $\theta = \theta_0$, $\varphi = \varphi_0$ and measure E_r as a function of r. Eq. (17) may then be written as

$$\sum_{n=1}^{N} c_n^{pw} G_n n(n+1) \Psi_n^1(kr) P_n^1(\cos\theta_0) = \frac{2rE_r(r)}{e^{i\varphi_0} + Ke^{-i\varphi_0}} \tag{35}$$

in which the summation has been truncated, now ranging from 1 to N instead of from 1 to infinity. Measuring $E_r(r)$ for N values of r therefore provides a set of N linear equations allowing one to determine experimentally N effective BSC G_ns. We believe that good criteria to determine both N and the discrete values of r_i ($i = 1, \ldots, N$) at which fields should be measured could be provided by the so-called localized approximation such as discussed in Refs. [15–17] for on-axis beams. Let us also note that the choice of θ_0 and φ_0 should not be made arbitrarily. For instance, if $\theta_0 = \pi/2$, we have $P_n^1(\cos\theta_0) = P_n^1(0)$, which is 0 for n even [18]. Therefore, for $\theta_0 = \pi/2$, only effective BSC G_ns, n odd, can be measured.

3.2 Using Cartesian Components

For $\theta = 0$, $\pi_n(\cos\theta)$ and $\tau_n(\cos\theta)$ are equal and finite. We then introduce

$$\pi_n(1) = \tau_n(1) = \Gamma_n. \tag{36}$$

From Eqs. (25) and (26), we then obtain

$$E_x(\theta = 0, \varphi = 0) = \frac{K+1}{2r} \sum_{n=1}^{\infty} c_n^{pw} G_n \Gamma_n \left(\frac{dr\Psi_n^1}{dr} - ikr\Psi_n^1 \right) \tag{37}$$

$$E_y(\theta = 0, \varphi = 0) = \frac{i(1-K)}{2r} \sum_{n=1}^{\infty} c_n^{pw} G_n \Gamma_n \left(\frac{dr\Psi_n^1}{dr} - ikr\Psi_n^1 \right). \tag{38}$$

Therefore, the polarization parameter K may be evaluated by using again Eq. (34), in which R now stands for the ratio $E_y(\theta = 0, \varphi = 0)/E_x(\theta = 0, \varphi = 0)$.
Next, let us consider (for instance) the component $E_x(r) = E_x(\theta = \varphi = 0)$, leading to

$$\sum_{n=1}^{\infty} c_n^{pw} G_n \Gamma_n \left(\frac{dr\Psi_n^1}{dr} - ikr\Psi_n^1 \right) = \frac{2rE_x(r)}{K+1}. \tag{39}$$

Therefore, similarly as in the previous subsection, N measurements of E_x (r), i.e. E_x on the beam axis, would allow one to determine N effective BSC G_ns.
Unfortunately, it is expected that field measurements would require complex experimental set-ups and, therefore, would appear to be difficult (although probably feasible). We must then investigate which kind of information can be retrieved from much easier intensity measurements.

4 Information Extracted from Intensity Measurements on Axisymmetric Beams

In this section, we again consider axisymmetric beams when BSCs satisfy Eq. (9), with $\epsilon = -1$, and Eq. (10). The longitudinal components S_z of the Poynting vector is then found to be (from Eqs. (8), (25), (26), (28) and (29))

$$S_z = \frac{k}{\omega\mu_0} E_0 E_0^* \frac{K^2+1}{4r^2} \mathrm{Re} \left[\cos\theta \sum_{n=1}^{\infty} \sum_{m=1}^{\infty} c_n^{pw} c_m^{pw*} g_n g_m^* A_n B_m^* + \sin\theta \sum_{n=1}^{\infty} \sum_{m=1}^{\infty} c_n^{pw} c_m^{pw*} g_n g_m^* m(m+1) B_n \Psi_m^1 P_m^1 \right] \tag{40}$$

in which we also used Eq. (14) and found it convenient to set

$$A_n = \frac{dr\Psi_n^1}{dr} \tau_n - ikr\Psi_n^1 \pi_n \tag{41}$$

$$B_n = \frac{dr\Psi_n^1}{dr} \pi_n - ikr\Psi_n^1 \tau_n. \tag{42}$$

We note that

$$(K^2+1) = (K+i)(K+i)^* \tag{43}$$

and define effective BSCs as

$$G_n = \sqrt{\frac{k}{\omega\mu_0}} E_0 (K+i) g_n \tag{44}$$

in a way slightly different to that for Eq. (13), leading to

$$S_z = \frac{1}{4r^2} \mathrm{Re}\left[\cos\theta \sum_{n=1}^{\infty}\sum_{m=1}^{\infty} c_n^{pw} c_m^{pw*} G_n G_m^* A_n B_m^* + \sin\theta \sum_{n=1}^{\infty}\sum_{m=1}^{\infty} c_n^{pw} c_m^{pw*} G_n G_m^* m(m+1) B_n \Psi_m^1 P_m^1 \right]. \tag{45}$$

We insert in Eq. (45) the expressions for A_n, B_n and c_n^{pw}, split double summations according to the parities of n and m and introduce the notations

$$\sum_n^{o} = \sum_{n=1}^{\infty} \quad , \text{n odd} \tag{46}$$

$$\sum_n^{e} = \sum_{n=1}^{\infty} \quad , \text{n even} \tag{47}$$

$$L_{nm} = \frac{2n+1}{n(n+1)} \frac{2m+1}{m(m+1)} \tag{48}$$

$$C_{nm}^1 = \frac{dr\Psi_n^1}{dr}\frac{dr\Psi_m^1}{dr} \tau_n \pi_m + k^2 r^2 \Psi_n^1 \Psi_m^1 \pi_n \tau_m \tag{49}$$

$$C_{nm}^2 = kr\left(\frac{dr\Psi_n^1}{dr}\Psi_m^1 \tau_n \tau_m - \frac{dr\Psi_m^1}{dr}\Psi_n^1 \pi_n \pi_m\right) \tag{50}$$

$$S_{nm}^1 = m(m+1)\Psi_m^1 \frac{dr\Psi_n^1}{dr} P_m^1 \pi_n \tag{51}$$

$$S_{nm}^2 = krm(m+1)\Psi_m^1 \Psi_n^1 P_m^1 \tau_n \tag{52}$$

$$G_{nm} = \mathrm{Re}(G_n G_m^*) \tag{53}$$

$$H_{nm} = \mathrm{Im}(G_n G_m^*). \tag{54}$$

Note that the matrices L_{nm}, C_{nm}^1, C_{nm}^2, S_{nm}^1 and S_{nm}^2 are real quantities. The matrix L_{nm} is symmetric, a property that we may denote by writing $L_{nm} = L_{(nm)} \cdot G_{nm}$ and H_{nm} are called partial density matrices. G_{nm} is symmetric, i.e. $G_{nm} = G_{(nm)}$, while H_{nm} is skew-symmetric, a property that we may denote by writing $H_{nm} = H_{[nm]}$. Eq. (45) then becomes

$$\begin{aligned} S_z = \frac{1}{4k^2r^2}\Bigg\{ &\left(\sum_n^{e}\sum_m^{e} - \sum_n^{o}\sum_m^{o}\right)(-1)^{(n+m)/2} L_{nm} \\ &\times [(\cos\theta\, C_{nm}^1 + \sin\theta\, S_{nm}^1) G_{nm} - (\cos\theta\, C_{nm}^2 - \sin\theta\, S_{nm}^2) H_{nm}] \\ &+ \left(\sum_n^{o}\sum_m^{e} - \sum_n^{e}\sum_m^{o}\right)(-1)^{(n+m-1)/2} L_{nm} \\ &\times [(\cos\theta\, C_{nm}^2 - \sin\theta\, S_{nm}^2) G_{nm} + (\cos\theta\, C_{nm}^1 \\ &+ \sin\theta\, S_{nm}^1) H_{nm}]\Bigg\}. \end{aligned} \tag{55}$$

This relation shows that we may measure experimentally the density matrices $G_{(nm)}$ and $H_{[nm]}$ and then obtain a density matrix:

$$I_{nm} = G_{nm} + iH_{nm} = G_n G_m^* \tag{56}$$

although the effective BSCs themselves cannot be measured. Eq. (55) will subsequently be used to produce sets of linear equations that one would solve in order to obtain density matrix elements, i.e. cross-products made out of BSCs. Therefore, it defines a linear inversion problem. As we may see, the BSCs phase information is lost when using such a linear algorithm, requiring the development of the so-called density matrix approach to GLMT (see Ref. [19], (Part 2)). However, starting from Eq. (40), we might define a nonlinear inversion problem. Algorithms for nonlinear inversions are more sophisticated than for linear inversions and will not be discussed in this paper. Let us mention, however, that they would allow one to determine the BSCs both in amplitude and phase (Polaert, personal communication). In any case, the set of relations to be inverted may be overdetermined, as usual in approximation problems. Details will be provided elsewhere together with actual numerical results. In this paper, we focus on the basic formulation. Effective algorithms for inversion require specific approaches and methods and their discussion is therefore postponed to future work. As a first instructive trial, let us specify $\theta = \pi/2$ so that Eq. (55) reduces to

$$\begin{aligned} S_z\left(\theta = \frac{\pi}{2}\right) = \frac{1}{4k^2r^2}\Bigg\{ &\left(\sum_n^{e}\sum_m^{e} - \sum_n^{o}\sum_m^{o}\right)(-1)^{(n+m)/2} L_{nm} \\ &\times (S_{nm}^1 G_{nm} + S_{nm}^2 H_{nm}) + \left(\sum_n^{o}\sum_m^{e} - \sum_n^{e}\sum_m^{o}\right) \\ &\times (-1)^{(n+m-1)/2} L_{nm} (S_{nm}^1 H_{nm} - S_{nm}^2 G_{nm})\Bigg\} \theta = \frac{\pi}{2}. \end{aligned} \tag{57}$$

However, we have [18]

$$\left.\begin{aligned} P_n^1(0) &\neq 0, \quad \text{n odd} \\ P_n^1(0) &= 0, \quad \text{n even} \end{aligned}\right\} \tag{58}$$

from which we derive

$$\left.\begin{aligned} \pi_n(0) &= P_n^1(0) \neq 0, \quad \text{n odd} \\ \pi_n(0) &= P_n^1(0) = 0, \quad \text{n even} \end{aligned}\right\} \tag{59}$$

$$\left.\begin{aligned} \tau_n(0) &\neq 0, \quad \text{n even} \\ \tau_n(0) &= 0, \quad \text{n odd} \end{aligned}\right\}. \tag{60}$$

It is then shown that $S_{nm}^1(\theta = \pi/2) = 0$ but for n and m odd and that $S_{nm}^2(\theta = \pi/2) = 0$ but for n even and m odd. Eq. (57) then simplifies to

$$\begin{aligned} S_z\left(\theta = \frac{\pi}{2}\right) = \frac{1}{4k^2r^2}\Bigg[&\sum_n^{e}\sum_m^{o}(-1)^{(n+m-1)/2} L_{nm} S_{nm}^2\left(\theta = \frac{\pi}{2}\right) G_{nm} \\ &- \sum_n^{o}\sum_m^{o}(-1)^{(n+m)/2} L_{nm} S_{nm}^1\left(\theta = \frac{\pi}{2}\right) G_{nm}\Bigg]. \end{aligned} \tag{61}$$

Therefore, measuring a profile $S_z(\theta = \pi/2)$ allows us to measure G_{nm}, n even, m odd from which we derive G_{nm}, n odd, m even since $G_{nm} = G_{(nm)}$, and also G_{nm}, n and m odd. However, we cannot retrieve any information concerning the components G_{nm}, n and m even or concerning the partial density matrix H_{nm}. Conversely, let us now measure an intensity profile S_z along the beam axis ($\theta = 0$). As we can see, all the information concerning the partial density matrices is contained in the beam axis only. Indeed, for $\theta = 0$, using Eqs. (49), (50) and (36) and introducing the real matrices:

$$D^1_{nm} = \frac{dr\Psi^1_n}{dr}\frac{dr\Psi^1_m}{dr} + k^2r^2\Psi^1_n\Psi^1_m \tag{62}$$

$$D^2_{nm} = kr\left(\frac{dr\Psi^1_n}{dr}\Psi^1_m - \frac{dr\Psi^1_m}{dr}\Psi^1_n\right). \tag{63}$$

Eq. (55) becomes

$$S_z(\theta = 0) = \frac{1}{4k^2r^2}\left[\left(\sum_n^e\sum_m^e - \sum_n^o\sum_m^o\right)(-1)^{(n+m)/2}L_{nm}\Gamma_n\Gamma_m\right.$$
$$(D^1_{nm}G_{nm} - D^2_{nm}H_{nm}) + \left(\sum_n^o\sum_m^e - \sum_n^e\sum_m^o\right)$$
$$\left.\times(-1)^{(n+m-1)/2}L_{nm}\Gamma_n\Gamma_m\left(D^2_{nm}G_{nm} + D^1_{nm}H_{nm}\right)\right]. \tag{64}$$

In Part 2 [19], devoted to the density matrix approach in generalized Lorenz-Mie theory, the polarization parameter K will also be needed. Eq. (55) shows that this parameter cannot be retrieved from S_z. Indeed, it has been incorporated in the definition of the effective BSCs G_n (Eq. (44)). Let us, however, evaluate the component S_x of the Poynting vector from Eqs. (8), (26), (27), (29) and (30), recalling that G_ns were there defined by Eq. (13). We obtain

$$S_x = \frac{E_0E_0^*}{4r^2}\frac{k}{\omega\mu_0}\mathrm{Re}\sum_{n=1}^{\infty}\sum_{m=1}^{\infty}\{(K^2+1)\cos\varphi c_n^{pw}c_m^{pw*}g_ng_m^*[\sin\theta B_nA_m^*$$
$$-m(m+1)\cos\theta P^1_m\Psi^1_mB_n] - i(1-K^2)\sin\varphi c_n^{pw}c_m^{pw*}g_ng_m^*n(n+1)$$
$$\times P^1_n\Psi^1_nA^*_m] \tag{65}$$

where A_n and B_n are defined by Eqs. (41) and (42).
Because $P^m_n(1) = 0$ [18], we see that $S_x(\theta = 0) = 0$, as we would have expected on physical grounds, therefore giving no information on K. Conversely, we may specify $\theta = \pi/2$, and evaluate (for instance)

$$S_x(\theta = \pi/2, \varphi = 0) = (K^2+1)\frac{E_0E_0^*}{4r^2}\frac{k}{\omega\mu_0}\mathrm{Re}\sum_{n=1}^{\infty}\sum_{m=1}^{\infty}c_n^{pw}c_m^{pw*}g_ng_m^*$$
$$B_n(0)A^*_m(0) \tag{66}$$

$$S_x(\theta = \pi/2, \varphi = \pi/2) = (K^2-1)\frac{E_0E_0^*}{4r^2}\frac{k}{\omega\mu_0}\mathrm{Re}\sum_{n=1}^{\infty}\sum_{m=1}^{\infty}$$
$$\times ic_n^{pw}c_m^{pw*}g_ng_m^*n(n+1)P^1_n(0)\Psi^1_nA^*_m(0). \tag{67}$$

We then insert Eq. (44) for the effective BSCs into Eqs. (66) and (67), yielding

$$S_x(\theta = \pi/2, \varphi = 0) = \frac{1}{4r^2}\mathrm{Re}\sum_{n=1}^{\infty}\sum_{m=1}^{\infty}c_n^{pw}c_m^{pw*}G_nG_m^*B_n(0)A^*_m(0) \tag{68}$$

which no longer depends on K, and.

$$S_x(\theta = \pi/2, \varphi = 0) = \frac{K^2-1}{K^2+1}\frac{1}{4r^2}\mathrm{Re}\sum_{n=1}^{\infty}\sum_{m=1}^{\infty}ic_n^{pw}c_m^{pw*}G_nG_m^*$$
$$n(n+1)P^1_n(0)\Psi^1_nA^*_m(0) \tag{69}$$

which does explicitly depend on K.
We then recall Eqs. (58)–(60), showing in particular that $A^*_m(0)$ are all different from zero:

$$\left.\begin{array}{ll} A^*_m(0) = ikr\Psi^1_m\pi_m(0), & \text{m odd} \\ A^*_m(0) = \frac{dr\Psi^1_m}{dr}\tau_m(0), & \text{m even}\end{array}\right\}. \tag{70}$$

We also use Eqs. (3), (48) and (53) to obtain eventually

$$S_x(\theta = \pi/2, \varphi = \pi/2) = \frac{K^2-1}{K^2+1}\frac{1}{4k^2r^2}\sum_n^o(-1)^{n/2}(2n+1)P^1_n(0)\Psi^1_n$$
$$\left[\sum_m^o(-1)^{m/2}\frac{2m+1}{m(m+1)}G_{nm}kr\Psi^1_m\pi_m(0) + \sum_m^e(-1)^{(m+1)/2}\frac{2m+1}{m(m+1)}\right.$$
$$\left.\times G_{nm}\frac{dr\Psi^1_m}{dr}\tau_m(0)\right] \tag{71}$$

which may be rewritten as

$$\frac{K^2-1}{K^2+1} = \frac{S_x(\theta = \pi/2, \varphi = \pi/2)}{R(r)} = \gamma(r) \tag{72}$$

in which R(r) is known since the partial density matrix G_{nm} has been evaluated previously. Measuring $S_x(\theta = \pi/2, \varphi = \pi/2)$ versus r therefore allows one to evaluate $\gamma(r)$ and to determine K^2 according to

$$K^2 = \frac{\gamma+1}{1-\gamma}. \tag{73}$$

In Eq. (72), we denoted γ as $\gamma(r)$ but the l.h.s. of this relation shows that it must be a constant. Departure of $\gamma(r)$ from constant values therefore may be due to R(r), indicating possibly that components G_{nm} have not been evaluated accurately enough, or that the number of evaluated components is not large enough. This relation therefore provides a possible test of convergence in the process of evaluating the partial density matrix G_{nm}. Also, other departures may be due to measurement errors in $S_x(\theta = \pi/2, \varphi = \pi/2)$. A fitting process on Eq. (73) would then improve the accuracy of the evaluation of K^2.
Now, because K is a real number [3], the sign of K, denoted ϵ_K, is still to be determined. This may be carried out by investigating field components by relying on modulus measurements, which is a practical way in so far as phases are then irrelevant. Furthermore, the determination of a sign is not very sensitive to measurement inaccuracies. An example of procedure is as follows.

From Eqs. (25) and (26), we have

$$E_x(\theta = \pi/2, \varphi = 0) = (K + 1)\mathcal{E} \tag{74}$$

$$E_y(\theta = \pi/2, \varphi = \pi/2) = i(1 - K)\mathcal{E} \tag{75}$$

in which

$$\mathcal{E} = \frac{E_0}{2r}\sum_{n=1}^{\infty} c_n^{pw} g_n n(n+1)\Psi_n^1 P_n^1(0). \tag{76}$$

We may then evaluate ϵ_K according to:

$$\left.\begin{aligned} &|E_x(\pi/2, 0)| > |E_y(\pi/2, \pi/2)\,| \Leftrightarrow \epsilon_K = +1 \\ &|E_y(\pi/2, \pi/2)| > |E_x(\pi/2, 0)\,| \Leftrightarrow \epsilon_K = -1 \end{aligned}\right\}. \tag{77}$$

As we stated previously, there is a redundancy between field components because they are linked by Maxwell's equations. Therefore, the above discussion certainly does not exhaust all opportunities. Furthermore, in many practical situations, the procedure may be simplified. For instance, let us assume that we are using a laser beam in the mode TEM_{00} (Gaussian beam), emanating from a polarized source. Then, as in the case of on-axis theoretical Gaussian beams, we may assume that $K = 1$ [3, 13, 14], so that only the partial density matrices have to be evaluated. Such evaluations may be needed to account for possible departures of the beam from the ideal Gaussian character, due, for instance, to the output aperture of the source, but still preserving the axisymmetric property of intensities (see example in Ref. [12]).

If the beam is indeed axisymmetric, as can be checked in the laboratory, we provide above a rigorous treatment of the problem of measuring BSCs, or associated quantities, in the laboratory. Any extra assumption could provide more opportunities (in so far as the assumptions are valid).

In this spirit, analysis of the beam in its Fraunhofer zone may allow one to evaluate approximately (but efficiently) the BSCs g_n themselves, both in amplitude and phase, from intensity measurements only [20]. The model developed in Ref. [20] allows one to reinterpret successfully the scattering experiments described in Ref. [12].

We now turn to the more general case of arbitrary-shaped beams described by a double set of BSCs $g^m_{n,TM}$, $g^m_{n,TE}$ for which no approximate approach, in the spirit of Ref. [20], has been available up to now.

5 Arbitrary-Shaped Beams

We only consider the extraction of information from intensity measurements. When the illuminating beam is encoded by a double set of BSCs, $g^m_{n,TM}$, $g^m_{n,TE}$, the BSPs (Eqs. (5) and (6)) and the field components obviously take more complicated forms than in the axisymmetric case [4]. Evaluating the component S_z of the Poynting vector, we establish, however, that [3]:

$$S_z = \frac{-E_0H_0^*}{2r^2}\,\mathrm{Re}\sum_{n=1}^{\infty}\sum_{m=-n}^{+n}\sum_{p=1}^{\infty}\sum_{q=-p}^{+p} i c_n^{pw} c_p^{pw*} e^{i(m-q)\varphi} \times [S_{np}^{mq}\sin\theta + C_{np}^{mq}\cos\theta] \tag{78}$$

in which

$$\begin{aligned} S_{np}^{mq} = kr[&-g^m_{n,TM}\, g^{q*}_{p,TM}\Psi_p(\Psi_n + \Psi_n'')P_n^{|m|}\tau_p^{|q|} + g^m_{n,TE} g^{q*}_{p,TE}\Psi_n \\ &\times(\Psi_p + \Psi_p'')P_p^{|q|}\tau_n^{|m|} + q g^m_{n,TM} g^{q*}_{p,TE}\Psi_p'(\Psi_n + \Psi_n'')P_n^{|m|}\pi_p^{|q|} \\ &+ m g^m_{n,TM} g^{q*}_{p,TE}\Psi_n'(\Psi_p + \Psi_p'')P_p^{|q|}\pi_n^{|m|}] \end{aligned} \tag{79}$$

$$\begin{aligned} C_{np}^{mq} = &- g^m_{n,TM} g^{q*}_{p,TM}\Psi_p\Psi_n'(\tau_n^{|m|}\tau_p^{|q|} + mq\pi_n^{|m|}\pi_p^{|q|}) \\ &+ g^m_{n,TM} g^{q*}_{p,TE}\Psi_n'\Psi_p'(m\pi_n^{|m|}\tau_p^{|q|} + q\pi_p^{|q|}\tau_n^{|m|}) \\ &- g^m_{n,TE} g^{q*}_{p,TM}\Psi_p\Psi_n(m\pi_n^{|m|}\tau_p^{|q|} + q\pi_p^{|q|}\tau_n^{|m|}) + g^m_{n,TE} g^{q*}_{p,TE} \\ &\Psi_n\Psi_p'(mq\pi_n^{|m|}\pi_p^{|q|} + \tau_n^{|m|}\tau_p^{|q|}) \end{aligned} \tag{80}$$

in which π_n^m and τ_n^m designate generalized Legendre functions:

$$\pi_n^m(\cos\theta) = \frac{P_n^m}{\sin\theta} \tag{81}$$

$$\tau_n^m(\cos\theta) = \frac{dP_n^m}{d\theta}. \tag{82}$$

We introduce three 4D arrays, again called density matrices, according to

$$M_{np}^{mq} = g^m_{n,TM} g^{q*}_{p,TM} \tag{83}$$

$$E_{np}^{mq} = g^m_{n,TE} g^{q*}_{p,TE} \tag{84}$$

$$C_{np}^{mq} = g^m_{n,TM} g^{q*}_{p,TE} \tag{85}$$

and three real quantities depending on r and θ:

$$\begin{aligned} F^{mq}_{np,M} = &- kr\sin\theta P_n^{|m|}\tau_p^{|q|}\Psi_p(\Psi_n + \Psi_n'') \\ &- \cos\theta\Psi_p\Psi_n'(\tau_n^{|m|}\tau_p^{|q|} + mq\pi_n^{|m|}\pi_p^{|q|}) \end{aligned} \tag{86}$$

$$\begin{aligned} F^{mq}_{np,E} = &kr\sin\theta\tau_n^{|m|}P_p^{|q|}\Psi_n(\Psi_p + \Psi_p'') + \cos\theta\Psi_n\Psi_p'(mq\pi_n^{|m|}\pi_p^{|q|} \\ &+ \tau_n^{|m|}\tau_p^{|q|}) \end{aligned} \tag{87}$$

$$\begin{aligned} F^{mq}_{np,C} = &kr\sin\theta[qP_n^{|m|}\pi_p^{|q|}\Psi_P'(\Psi_n + \Psi_n'') + m\pi_n^{|m|}P_p^{|q|}\Psi_n'(\Psi_p + \Psi_p'')] \\ &+ \cos\theta(m\pi_n^{|m|}\tau_p^{|q|} + q\tau_n^{|m|}\pi_p^{|q|})(\Psi_n\Psi_p + \Psi_n'\Psi_p'). \end{aligned} \tag{88}$$

Let us also use the usual normalization condition of GLMT [4]:

$$\frac{1}{2}E_0H_0^* = 1 \tag{89}$$

or, equivalently, let us absorb $E_0H_0^*/2$ into the density matrices. Then, Eq. (78) can be written as

$$S_z = \frac{-1}{r^2}\,\mathrm{Re}\; i\sum_{n=1}^{\infty}\sum_{m=-n}^{+n}\sum_{p=1}^{\infty}\sum_{q=-p}^{+p} c_n^{pw} c_p^{pw*} e^{i(m-q)\varphi} \times [M_{np}^{mq}F^{mq}_{np,M} + E_{np}^{mq}F^{mq}_{np,E} + C_{np}^{mq}F^{mq}_{np,C}]. \tag{90}$$

Let us specify the expression for c_n^{pw} (Eq. (3)), introduce L_{nm} (Eq. (48)) and set

$$e^{i(m-q)\varphi} = \varphi_{mq} + i\gamma_{mq} \tag{91}$$

where φ_{mq} and γ_{mq} are real numbers.
Eq. (90) then can be converted into

$$\begin{aligned} S_z = \frac{-1}{k^2r^2}\Bigg\{ & \left(\sum_n^e\sum_p^o - \sum_n^o\sum_p^e\right) L_{np}(-1)^{(n+p-1)/2} \\ & \times \sum_m\sum_q \gamma_{mq} I_{np}^{mq} + \left(\sum_n^o\sum_p^o - \sum_n^e\sum_p^e\right) L_{np}(-1)^{(n+p)/2} \\ & \sum_m\sum_q \varphi_{mq} I_{np}^{mq} + \left(\sum_n^o\sum_p^e - \sum_n^e\sum_p^o\right) L_{np}(-1)^{(n+p-1)/2} \\ & \sum_m\sum_q \varphi_{mq} R_{np}^{mq} + \left(\sum_n^o\sum_p^o - \sum_n^e\sum_p^e\right) L_{np}(-1)^{(n+p)/2} \\ & \sum_m\sum_q \gamma_{mq} R_{np}^{mq}\Bigg] \end{aligned} \tag{92}$$

in which

$$I_{np}^{mq} = \mathrm{Im}(M_{np}^{mq})F_{np,M}^{mq} + \mathrm{Im}(E_{np}^{mq})F_{np,E}^{mq} + \mathrm{Im}(C_{np}^{mq})F_{np,C}^{mq} \tag{93}$$

$$R_{np}^{mq} = \mathrm{Re}(M_{np}^{mq})F_{np,M}^{mq} + \mathrm{Re}(E_{np}^{mq})F_{np,E}^{mq} + \mathrm{Re}(C_{np}^{mq})F_{np,C}^{mq}. \tag{94}$$

Investigation of Eqs. (92)–(94) then reveals that measuring $S_z(r)$ for θ and φ fixed in principle allows the evaluation of density matrix components by solving a linear inversion problem (again, it will be worthwhile in future work to examine the opportunities offered by using nonlinear inversion techniques). All values of θ and φ are not allowed, however. For instance, if $\theta = 0$, considering the properties of the generalized Legendre functions π_n^m and τ_p^q, it is found that only components with $|m|$ and $|q|$ equal to $+1$ may be involved [3]. Similarly, it may be demonstrated that many components are not available if we take $\theta = \pi/2$. Many other opportunities are hidden in Eq. (92) and systematic numerical studies should help to select the most efficient ones.
If the beam is axisymmetric, however, the present general procedure could also be used, but it would be also valid to use it for $\theta = 0$ since only BSCs g_n^m with $m = \pm 1$ are then different from 0. Therefore, we are faced with 12 density submatrices M_{np}^{11}, $M_{np}^{1-1}, \ldots, C_{np}^{-11}, C_{np}^{-1-1}$. Owing to the properties of axisymmetric beams (Eq. (9)), we may reduce the number of necessary matrices. For instance, we obtain

$$M_{np}^{11} = \frac{I_{np}}{8(K^2+1)} \tag{95}$$

in which we have used the normalization condition (89) under the equivalent form

$$\frac{1}{2}\frac{k}{\omega\mu_0}E_0E_0^* = 1. \tag{96}$$

We then see that the price to pay for the reduction from 12 density submatrices to a single density matrix is the introduction of the polarization parameter K.

6 Conclusion

It has been demonstrated that beam shape coefficients appearing in the generalized Lorenz-Mie theory, or at least associated quantities, may be experimentally measured on actual beams in the laboratory, rather than derived from *a priori* theoretical beam models. The most important results in this paper concern the analysis of intensity measurements. In the case of axisymmetric beams, we may evaluate two partial density matrices G_{nm} and H_{nm} from which we may form a single density matrix I_{nm}. In the most general case, when the incident beam is encoded by a double set of beam shape coefficients $g_{n,TM}^m$, $g_{n,TE}^m$, we introduced three 4D density matrices M_{np}^{mq}, E_{np}^{mq}, C_{np}^{mq}, which may also be evaluated from intensity measurements. When the beam is axisymmetric, the three 4D density matrices degenerate to 12 2D submatrices which, by introducing a scalar real polarization parameter, degenerate further to the single density matrix I_{nm}.
Interest in these matrices is only warranted if a significant amount of the GLMT may be rewritten in terms of them, rather than in terms of the beam shape coefficients. This issue is investigated in Part 2 in which the GLMT is expressed in the so-called density matrix approach. We shall then also justify the density matrix terminology when the whole framework is completed.
The contents of this paper (together with the contents of Part 2) then offer new opportunities for refined particle characterizations when the actual beam used in the laboratory departs from an ideal beam such as that described by an *a priori* mathematical model. Even if laser beams are properly created at the source level, they may afterwards be significantly disturbed by the subsequent optical system used. Therefore, some scattering phenomena used for particle characterizations should preferably be described by measuring the shaped beam coefficients, and subsequently entering them in the GLMT framework.

7 Addendum

During the submission process of this paper, algorithms began to be implemented to produce effective results. It then appeared that the algorithms described in this paper are indeed effective. It has also be revealed that using nonlinear rather than linear inversion techniques would allow to determine the BSCs, both in amplitude and phase, therefore extending further the opportunities offered by the present work (Polaert, personal communication).

8 Symbols and Abbreviations

A_n	Eq. (41)
B_n	Eq. (42)
BSC	beam shape coefficient
BSP	Bromwich scalar potential
C_{nm}^1	Eq. (49)
C_{nm}^2	Eq. (50)
C_{np}^{mq}	cross-density-matrix or Eq. (80)
c_n^{pw}	expansion coefficients in Lorenz-Mie theory
E_0	electric strength
E_i	electric field components
E_{np}^{mq}	TE density matrix
$F_{np,M}^{mq}$	Eq. (86)
$F_{np,E}^{mq}$	Eq. (87)

$F^{mq}_{np,C}$	Eq. (88)
g_n	beam shape coefficients (axisymmetric beams)
G_n	effective beam shape coefficients, Eq. (13) or (44)
G_{nm}	partial density matrix, real part of the density matrix I_{nm}
$g^m_{n,TM} g^m_{n,TE}$	beam shape coefficients (arbitrary-shaped beams)
GLMT	generalized Lorenz-Mie theory
H_i	magnetic field components
H_0	magnetic strength
H_{nm}	partial density matrix, imaginary part of the density matrix I_{nm}
I_{nm}	density matrix (axisymmetric beams)
I^{mq}_{np}	Eq. (93)
k	wavenumber
K	polarization parameter
L_{nm}	Eq. (48)
M^{mq}_{np}	TM density matrix
P^m_n	associated Legendre polynomials
R^{mq}_{np}	Eq. (94)
S_i	Poynting vector
S^1_{nm}	Eq. (51)
S^2_{nm}	Eq. (53)
S^{mq}_{np}	Eq. (79)
TE	transverse electric
TM	transverse magnetic
U_{TE}	transverse electric BSP
U_{TM}	transverse magnetic BSP
(r, θ, φ)	spherical coordinates
(x, y, z)	Cartesian coordinates
ϵ	± 1
ϵ_K	sign of the polarization parameter
ϵ_0, μ_0	electric and magnetic capacities of the free space
π_n, τ_n	Legendre functions
π^m_n, τ^m_n	generalized Legendre functions
θ_0	special value of θ
φ_0	special value of φ
φ_{mq}	real part of exp $[i(m-q)\varphi]$
γ_{mq}	imaginary part of exp $[i(m-q)\varphi]$
Γ_n	Eq. (36)
ω	angular frequency
Ψ^1_n	spherical Bessel functions
Ψ_n	Ricatti-Bessel functions

9 References

[1] *G. Gouesbet:* Generalized Lorenz-Mie theory and applications. Part. Part. Syst. Charact. *11* (1994) 22–34.

[2] *F. Onofri, G. Gréhan, G. Gouesbet:* Electromagnetic scattering from a multilayered sphere located in an arbitrary beam. Appl. Opt. *34* (1995) 7113–7124.

[3] *G. Gouesbet*: Partial wave expansions and properties of axisymmetric light beams. Appl. Opt. *35* (1996) 1543–1555.

[4] *G. Gouesbet, B. Maheu, G. Gréhan*: Light scattering from a sphere arbitrarily located in a Gaussian beam, using a Bromwich formulation. J. Opt. Soc. Am. A, *5* (1988) 1427–1443.

[5] *J. A. Lock, G. Gouesbet:* A rigorous justification of the localized approximation to the beam shape coefficients in generalized Lorenz-Mie theory: I. On axis beams. J. Opt. Soc. Am. A, *11* (1994) 2503–2515.

[6] *G. Gouesbet, J. A. Lock:* A rigorous justification of the localized approximation to the beam shape coefficients in generalized Lorenz-Mie theory, II. Off-axis beams. J. Opt. Soc. Am. A, *11* (1994) 2516–2525.

[7] *G. Gouesbet, C. Letellier, K. F. Ren, G. Gréhan*: Discussion of two quadrature methods of evaluating beam shape coefficients in generalized Lorenz-Mie theory. Appl. Opt. *35* (1996) 1537–1542.

[8] *K. F. Ren, G. Gréhan, G. Gouesbet*: Electromagnetic field expression of a laser sheet and the order of approximation. J. Opt. (Paris) *25* (1994) 165–176.

[9] *K. F. Ren, G. Gréhan, G. Gouesbet*: Evaluation of laser sheet beam shape coefficients in generalized Lorenz-Mie theory by using a localized approximation. J. Opt. Soc. Am. A, *11* (1994) 2072–2079.

[10] *K. F. Ren, G. Gréhan, G. Gouesbet*: Laser sheet scattering by spherical particles. Part. Part. Syst. Charact. *10* (1993) 146–151.

[11] *G. Gouesbet, J. A. Lock, G. Gréhan*: Partial wave representations of laser beams for use in light scattering calculations. Appl. Opt. *34* (1995) 2133-2143.

[12] *J. T. Hodges, G. Gréhan, G. Gouesbet, C. Presser*: Forward scattering of a Gaussian beam by a nonabsorbing sphere. Appl. Opt. *34* (1995) 2120–2132.

[13] *G. Gouesbet, G. Gréhan*: Sur la généralisation de la théorie de Lorenz-Mie. J. Opt. (Paris) *13* (1982) 97–103.

[14] *G. Gouesbet, G. Gréhan, B. Maheu:* Scattering of a Gaussian beam by a Mie scatter center, using a Bromwich formulation. J. Opt. Paris *16* (1985) 83–93. Republished in selected papers on light scattering, SPIE Milestone Series, Vol. 951, edited by M. Kerker, Part I, (1988) 361–371.

[15] *G. Gréhan, B. Maheu, G. Gouesbet:* Scattering of laser beams by Mie scatter centers: numerical results using a localized approximation. Appl. Opt. *25* (1986) 3539–3548.

[16] *B. Maheu, G. Gréhan, G. Gouesbet:* Generalized Lorenz-Mie theory: first exact values and comparisons with the localized approximation. Appl. Opt. *26* (1987) 23–26.

[17] *G. Gouesbet, G. Gréhan, B. Maheu:* Computations of the coefficients g_n in the generalized Lorenz-Mie theory using three different methods. Appl. Opt. *27* (1988) 4874–4883.

[18] *L. Robin:* Fonctions sphériques de Legendre et fonctions sphéroïdales, Gauthier-Villars, Paris, 1957–1959. Vols. 1–3.

[19] *G. Gouesbet:* Measurements of beam shape coefficients in generalized Lorenz-Mie theory and the density-matrix approach. Part 2: Density-matrix approach. Part. Part. Syst. Charact. *14* (1997) in press.

[20] *J. A. Lock, J. T. Hodges:* Far field scattering of an axisymmetric laser beam of arbitrary profile by an on-axis spherical particle. Appl. Opt., to be published.